ACS OMEGA

Open Access

http://pubs.acs.org/journal/acsodf

Article

Nanocellulose@gallic Acid-Based MOFs: A Novel Material for Ecofriendly Food Packaging

Raveena and Pratibha Kumari*

Cite This: *ACS Omega* 2024, 9, 35654−35665

Read Online

ACCESS | Metrics & More | Article Recommendations | Supporting Information

ABSTRACT: The development of an effective food packaging material is essential for safeguarding against infections and preventing chemical, physical, and biological changes during food storage and transportation. In the present study, we successfully synthesized an innovative food packaging material by combining chitosan (CH), nanocellulose (NC), and a gallic acid-based metal−organic framework (MOF). The CH films were prepared using different concentrations of NC (5 and 10%) and MOFs (1.5, 2.5, and 5%). Various properties of prepared films, including water solubility (WS), moisture content (MC), swelling degree, oxygen permeability, water vapor permeability (WVP), mechanical property, color analysis, and light transmittance, were studied. The chitosan film with a 5% NC and 1.5% MOF (CH-5% NC-1.5% MOF) exhibited the least water solubility, moisture content, and water vapor permeability, indicating the overall stability of the film. Additionally, this film demonstrated low oxygen permeability, as indicated by a peroxide value of 18.911 ± 4.009, ensuring the effective preservation of packaged contents. Notably, this synthesized film exhibited high antioxidant activity, resulting in an extended duration of 52 days. This antioxidant activity was further validated by the preservation of apple slices for 9 days in a CH-5% NC-1.5% MOF film. The findings of the study suggest that the developed films can provide a promising and environmentally friendly solution for active food packaging.

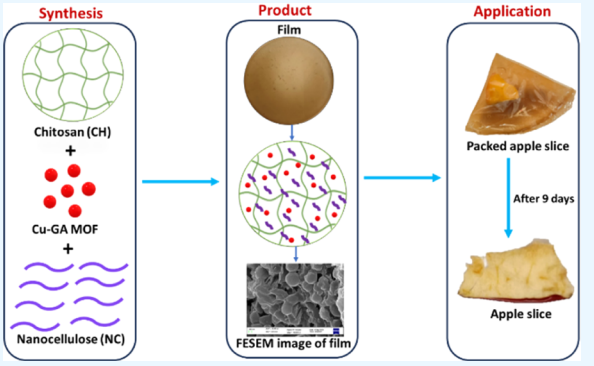

1. INTRODUCTION

Food packaging plays a vital role in preserving food quality and safeguarding it throughout various stages, such as processing, distribution, and storage within the food supply chain. According to the 2022 report by Allied Market Research (code A01964), the global packaging market value was $966.72 billion in 2021, and it is expected to reach $1464.35 billion by 2031 with an increase of 4.3% in the compound annual progress rate (CAGR).[1] The most popular packaging material is plastic because it is lightweight, easily processed, has a low cost of production, and has excellent mechanical and barrier properties.[2] In 2022, the worldwide value of plastic packaging reached $369.21 billion, and it is expected to expand at a CAGR of 3.6% by 2030.[3] However, despite its popularity, there is an increasing concern regarding plastic as it takes centuries to degrade.[4] Moreover, the recycling rate of plastics is 14−18%, which is very low compared to other materials such as metal, glass, and paper.[5] Due to the low recycling rate, 6300 million tons of plastic waste have been generated since 1950, and 4977 million plastic wastes have been accumulated in landfills and waterbodies.[4] Moreover, the emergence of microplastics in the air, water, and soil poses a significant threat to both terrestrial and marine ecosystems.[6]

Recently, research interests have been growing toward the development of biodegradable and sustainable packaging material that can increase the shelf life of packaged food.[7] These demands inspired to develop active food packaging films, which can prevent the deterioration of food products by microbial contamination, off-flavor development, oxidation, texture breakdown, and can provide efficient moisture and gas-barrier properties.[8] Biopolymers have been used in making active packaging materials as they are renewable, abundant in nature, low cost, ecofriendly, and biodegradable.[9] The chitosan (CH) biopolymer is the commonly used active food packaging component due to its good film-forming properties, antimicrobial activity, nontoxicity, and biocompatibility.[10] However, it offers some limitations such as poor water resistance, low mechanical properties, brittle nature, and low thermal stability.[11] Further, the mechanical, barrier, and thermal properties of the CH film can be enhanced by incorporating various inorganic and organic nanomaterials.[12]

Nanocellulose (NC) has emerged as a prominent biobased nanomaterial drawing escalating research interests due to its exceptional physicochemical properties, biodegradability, bio-

Received: April 22, 2024
Revised: July 2, 2024
Accepted: July 17, 2024
Published: July 27, 2024

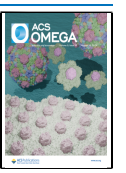

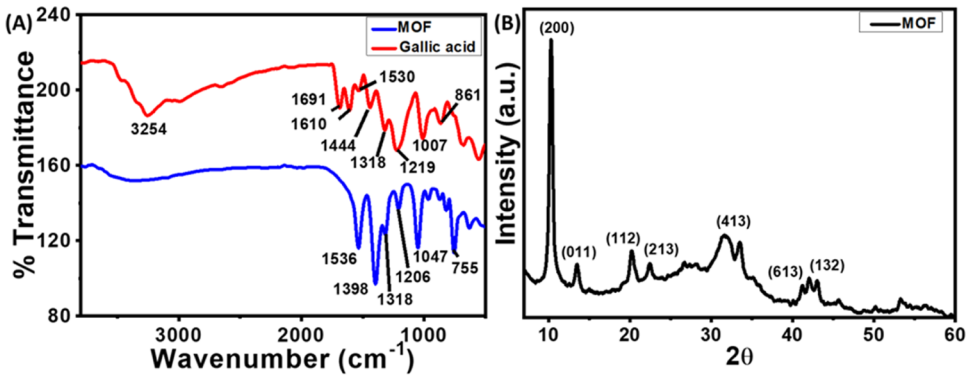

Figure 1. (A) FTIR spectra and (B) powder-XRD data of the MOF.

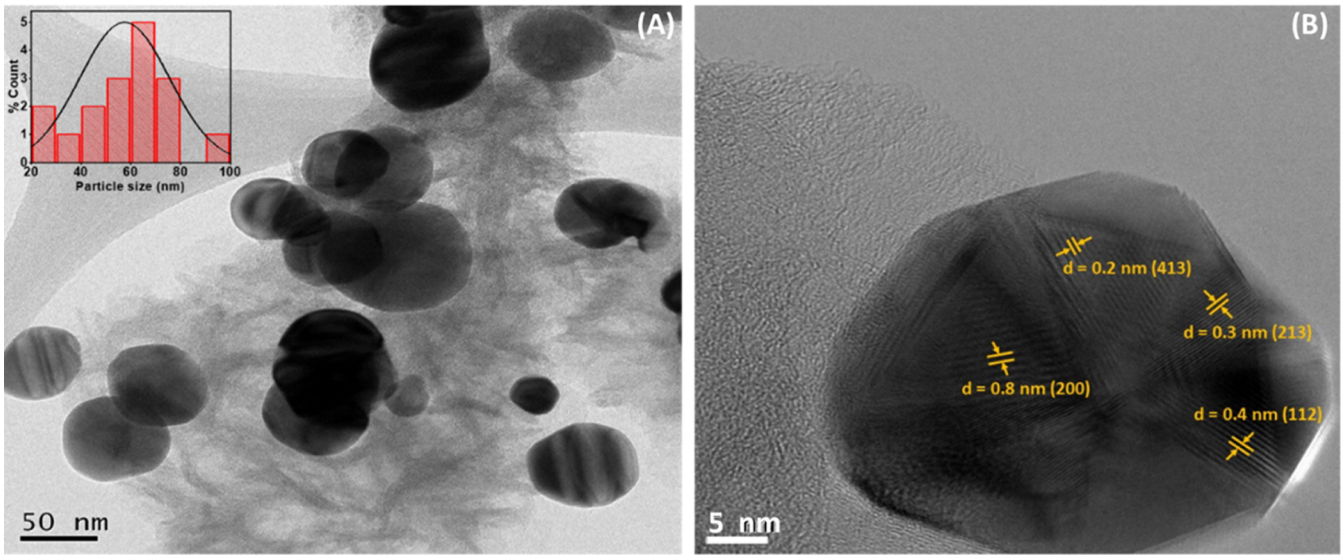

Figure 2. TEM image of the MOF at different scales: (A) 50 nm and (B) 5 nm.

compatibility, and high abundance.[13] The combination of CH, glycerol, and NC can create strong and dense surfaces due to strong H-bonding interactions, which is impermeable to molecules and hence provides excellent barrier properties in the CH−NC film as desired for a good food packaging material.[12,14,15] However, the CH−NC film cannot exhibit antioxidant activity, which can prevent the deterioration of the food.

There are few reports regarding the enhancement of the antioxidant activity of CH- and NC-based films by incorporating naturally occurring plant phenolic compounds and also contributing to human health.[16] Freire et al. demonstrated that the addition of ferulic acid or feruloylated arabinoxylo-oligosaccharides to nanocomposite films significantly increased their antioxidant activity.[17] Gaikwad et al. found that the addition of litchi shell waste extract to guar gum/carboxymethyl cellulose films improved their antioxidant properties.[18] Feng et al. found that the addition of epigallocatechin-3-gallate in the CH-bacterial NC-based active film exhibited good antioxidant properties.[19] Rhim et al. further enhanced the antioxidant activity of carboxymethyl cellulose films by incorporating curcumin and zinc oxide.[20] However, gallic acid is a low-molecular-weight compound shown to possess strong antioxidant activity in many studies.[21] Due to the advantages of gallic acid, many scientists incorporated it into the CH and CH−NC film. Vilela et al. enhanced the antioxidant property by adding gallic acid in a starch and bacterial NC-based active film.[22] Scientists synthesized a gallic-acid-grafted CH film, which exhibited high antioxidant and physical properties as compared to a pure CH film.[16,23−25] The gallic-acid-grafted CH film was used to preserve *Agaricus bisporus*, which increases the antioxidant status and maintains the postharvest quality.[26] However, these reported materials possess certain drawbacks, such as their antioxidant activity for a limited time, reduced oxygen barrier capacity, and inadequate thermal stability. Therefore, there is a necessity to improve the antioxidant efficacy, thermal stability, and reduction in oxygen permeability of the packaging film material for an extended period.

A gallic-acid-based metal−organic framework (MOF) has been used in diverse areas due to its high surface area, high thermal stability, high antioxidant properties, sustained release of antioxidants, and high adsorption properties.[27] It was utilized for drug delivery, and it demonstrated approximately 85% cell viability in Panc-1 cells and was also tested on the Ehrlich-Lettre Ascites Carcinoma (EAC) cancer cell line, indicating its nontoxicity to human beings.[28] However, gallic-acid-based MOFs have not been used in food packaging films. Herein, we report on synthesizing a CH−NC film modified with a gallic-based MOF for food packaging applications. Various properties of the developed film, such as oxygen permeability, water vapor permeability (WVP), water

https://doi.org/10.1021/acsomega.4c03847
ACS Omega 2024, 9, 35654−35665

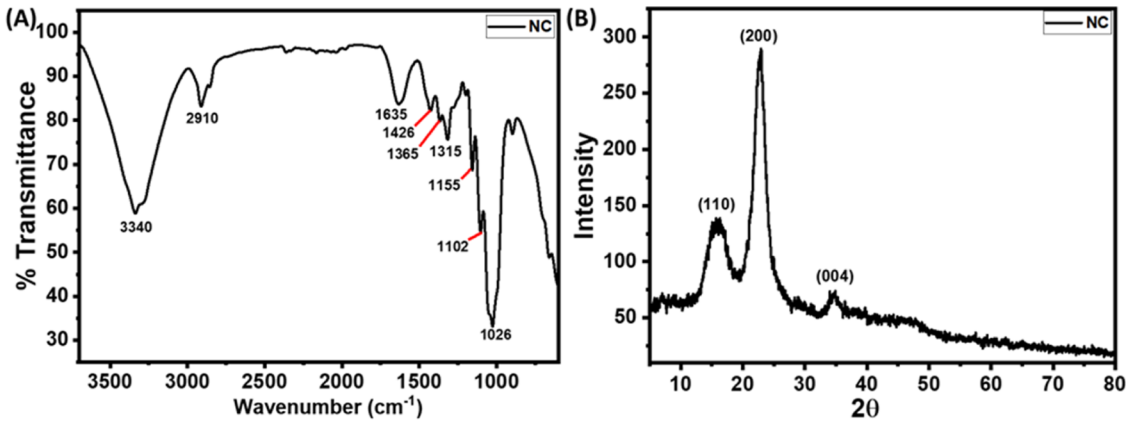

Figure 3. (A) FTIR spectrum and (B) powder-XRD data of synthesized NC.

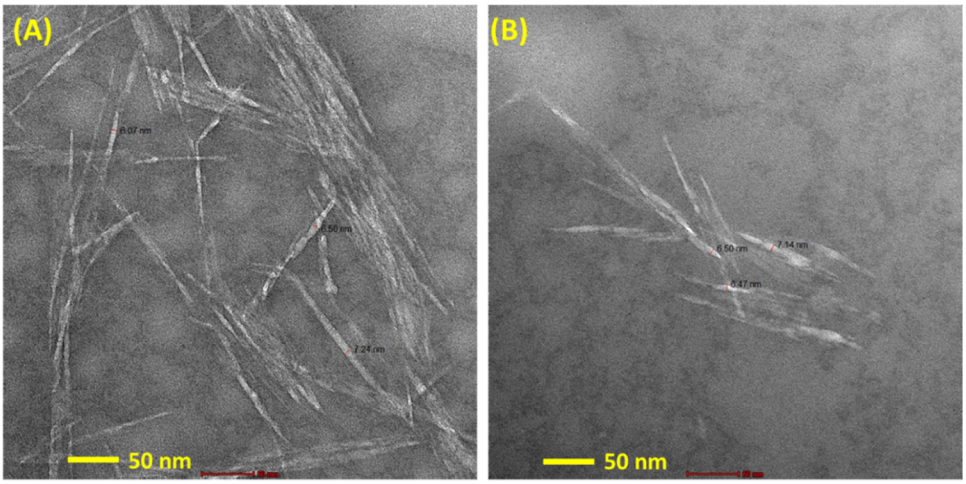

Figure 4. (A, B) TEM images of NC at the 50 nm scale.

solubility, mechanical property, optical property, and antioxidant nature, have been studied.

2. RESULTS AND DISCUSSION

2.1. Synthesis and Characterization of the MOF. A gallic acid-based metal−organic framework (MOF) was prepared using the micelle approach.[28] In the FTIR spectra of the MOF, the peaks at 1536 and 1398 cm^{-1} corresponded to the asymmetric and symmetric stretching vibration of C−O of the carboxylate group (OCO−), respectively (Figure 1A). The presence of peaks at 1318, 1206, and 1047 cm^{-1} can be ascribed to the stretching of C−O of the phenolic group. The Cu−O stretching vibration appeared at 755 cm^{-1}. Further, the O−H stretching vibration peak at 3500−3260 cm^{-1} and the carbonyl group stretching peak at 1691 cm^{-1} disappeared, which were present in the gallic acid, indicating the involvement of hydroxyl and carboxylic groups of gallic acid in the binding with the metal ion.[28]

The crystalline structure of the MOF was confirmed by the powder-XRD pattern. In the powder XRD (Figure 1B), the diffraction peaks appeared at 2θ = 10.26, 13.46, 20.23, 22.39, 31.49, 41.28, and 43.04°, corresponding to the (200), (011), (112), (213), (413), (613), and (132) diffraction planes, respectively, which supported the synthesis of the MOF.[27] The morphology of the MOF was examined by TEM images. In the TEM images, the MOF appeared to have a spherical shaped structure (Figure 2). Energy-dispersive X-ray analysis (EDAX) showed the presence of carbon, oxygen, and copper in the MOF (Figure S4). The stability of the MOF was examined by the TGA data (Figure S5). Initially, there was loss of water/moisture from the surface of the material in the temperature range of 42−110 °C with a 3.72% weight loss. In the temperature range of 111−584 °C, a 39.84% weight loss was observed, which may be due to the decomposition of the gallic acid unit. After that, stabilization occurred due to the production of copper oxide.[27,28]

2.2. Synthesis and Characterization of Synthesized TEMPO-Oxidized NC. Cellulose was extracted from wheat straw and was oxidized by TEMPO and NaBr to prepare nanocellulose (NC) (Figure S6).[29,30] The degree of oxidation was determined by conductometric titration (Figure S7),[31] and it was found to be 32.60%.

The synthesized NC was characterized by FTIR spectroscopy, powder-XRD, FESEM, and EDAX. In the FTIR spectrum (Figure 3A), the peaks at 3340, 2910, and 1635 cm^{-1} corresponded to the O−H bond, sp^3-hybridized C−H bond, and C═O bond of the carboxylate group, respectively.[32,33] The peaks that appeared at 1426, 1365, and 1315 cm^{-1} may be ascribed to CH_2 bending, C−H bending, and CH_2 rocking, respectively.[34,35] The peak present at 1155, 1102, and 1026 cm^{-1} corresponded to the C−C ring bond, the glycosidic ether bond, and the C−O−C bond (pyranose ring of cellulose), respectively.[36] In the powder-XRD pattern, sharp diffraction peaks were present at 2θ values of 16.21, 22.80, and

https://doi.org/10.1021/acsomega.4c03847
ACS Omega 2024, 9, 35654−35665

34.87° for the planes (110), (200), and (004),[37] respectively (Figure 3B). It indicated the crystallinity of NC. The morphology of NC was examined by FESEM images (Figure S8) and TEM images (Figure 4). The NC looked like fibers with a thickness ranging between 6 and 8 nm (Figure 4).[38] In the EDAX, carbon, oxygen, and sodium elements were present with weight percent of 77.46, 18.04, and 4.50, respectively (Figure S9).

2.3. Characterization of Synthesized CH−NC−MOF Films. The CH−NC−MOF films (Figure S10) were prepared with different amounts of CH, NC, and MOF by modifying the reported method.[19] The prepared films were characterized by different techniques, such as FTIR, powder-XRD, FESEM, and TGA.

The FTIR spectra of pure chitosan exhibited two bands at 3361 and 3291 cm^{-1} due to O−H and N−H stretching vibrations (Figure 5).[39] The stretching bands at 2931 and 2883

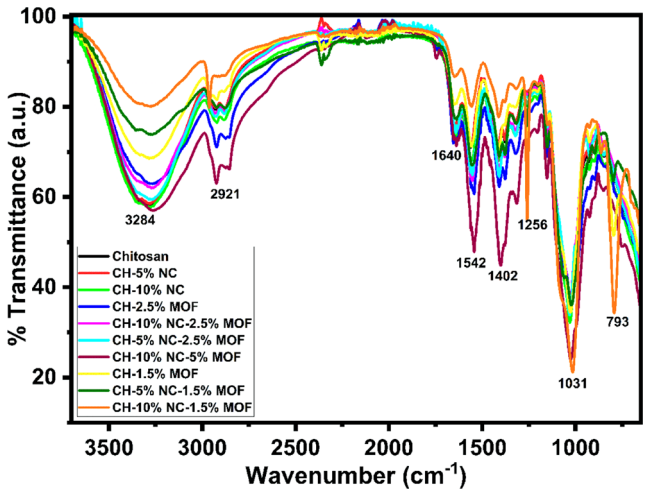

Figure 5. FTIR spectra of all synthesized CH−NC−MOF films.

cm^{-1} were associated with the C−H stretching bond of the CH_2 and CH_3 groups of the glucosamine unit of CH.[40] The bands exhibited at 1643, 1564, 1417, 1377, 1322, 1147, and 1028 cm^{-1} are attributed to the C═O stretching vibration, N−H bending vibration, $-CH_2$ scissoring, $-CH_3$ deformation band, C−N stretching of amide, C−O−C band stretching, and C−O stretching, respectively.[41−43] After the addition of NC and the MOF in the CH film, the O−H peak shifted toward a lower frequency, indicating the H-bonding interaction of CH with NC, and a new peak appeared at 793 cm^{-1} due to the Cu−O stretching vibration of the MOF.[44]

The powder-XRD pattern of the CH film exhibited a sharp diffraction peak at 2θ = 21.53° for the (110) plane due to the hydrated crystalline structure of the polymer (Figure 6).[45,46] Two low intense peaks appeared at 2θ values of 9.45 and 13.77°. Upon integration of NC and MOF into the CH film, the distinct sharp peak for the (110) plane became broader and exhibited a slight shift. There was a shift in the 2θ value from 19.0 to 22.54° when 5% NC was added to the CH film, and it further shifted to 21.19° with 10% NC in the CH film. The incorporation of the MOF also affected the diffraction peak as it shifted to 20.52° with a 1.5% MOF and to 22.54° with a 2.5% MOF in the CH film. More shifting was observed in the CH-5% NC-1.5% MOF and CH-10% NC-2.5% MOF films from 19.0 to 22.61° and to 23.56°, respectively (Figure 6). The broadness in the peak indicated a reduction in the crystallinity

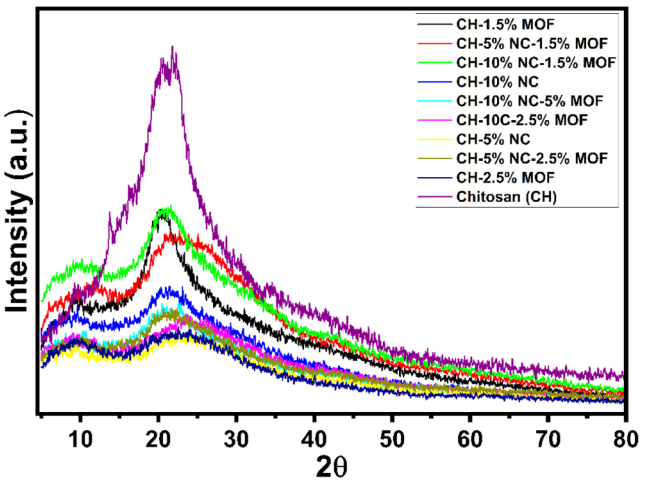

Figure 6. Powder-XRD data of all synthesized CH−NC−MOF films.

of the compound by the hydrogen-bonding interaction between the components.[47] The shifts in the diffraction peaks were ascribed to the presence of NC and the MOF, with their respective peaks occurring at 22.80 and 22.39°, indicating significant intercomponent interactions.[45] Interestingly, the characteristic peaks of NC and the MOF were absent in the powder-XRD spectra of the composite films, likely due to their lower concentrations relative to CH.[45,48]

The morphology of the prepared films was observed by surface and cross-sectional FESEM analysis. In the FESEM images, the smooth morphology of the CH film was affected after incorporating NC and the MOF, and it became rough, porous, and dense. When the NC and MOF concentration was increased, the aggregation appeared, and it was observed in cross-sectional FESEM images (Figure 7). A similar observation has been reported in another study.[19,49] Overall, the FESEM images clearly illustrated how varying concentrations of NC and MOF affected film morphology, elucidating their individual and combined effects on the microstructure (Figure S11).[49,50] The thickness of the synthesized films was determined by the cross-sectional FESEM images because the cross-sectional FESEM is a common and efficient technique to examine the morphology as well as film thickness.[51−54] The thickness of films was measured at 5 different positions, and their mean ± standard deviation values are given in Table 1. The thickness of the CH film increased after the incorporation of NC and the MOF due to increased solid content in the film.[20]

The TGA curves of all synthesized films are shown in Figure S12. The weight losses of the films were observed in 3 steps. The initial volatilization of water molecules occurred in the temperature range between 90 and 120 °C.[55] Two significant mass losses were observed in the temperature range of 120−210 and 210−280 °C due to the degradation of glycerol and CH, respectively.[55] Notably, the inherent stability of the CH film was relatively low, but the film's stability improved after the addition of 5% NC because NC decomposed in the temperature range of 240−350 °C.[56] This upgrade implies that the addition of NC strengthened the structure of the film and increased its thermal stability.[57] When the MOF was incorporated in the CH−NC film, the weight loss decreased in the temperature range from 90 to 230 °C because of high cross-linking between the components.[58] The main degradation of the CH−NC−MOF film was noticed in the

https://doi.org/10.1021/acsomega.4c03847
ACS Omega 2024, 9, 35654−35665

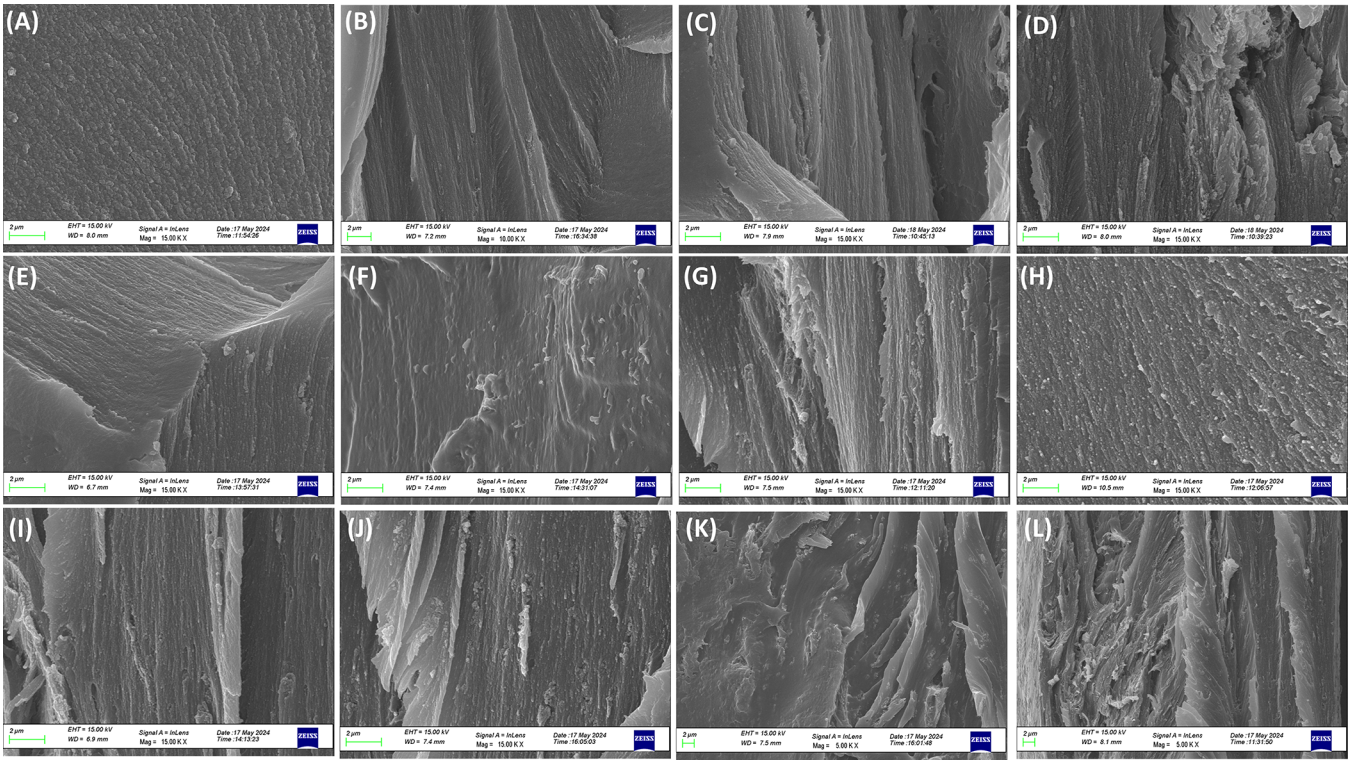

Figure 7. Cross-sectional FESEM images of the synthesized films: (A) chitosan (CH), (B) CH-5% NC, (C, D) CH-10% NC, (E) CH-1.5% MOF, (F) CH-2.5% MOF, (G, H) CH-5% NC-1.5% MOF, (I) CH-10% NC-1.5% MOF, (J) CH-5% NC-2.5% MOF, (K) CH-10% NC-2.5% MOF, and (L) CH-10% NC-5% MOF.

Table 1. Obtained Results of Thickness, MC, WS, SD, PV Value, and WVP of the Synthesized Films

s.no.	film	thickness (μm)	% MC	% WS	% SD	PV (meq/kg)	WVP (g h^{-1} m^{-2})
1.	chitosan (CH)	62.05 ± 1.95	21.40 ± 1.60	37.98 ± 0.88	50.50 ± 3.94	63.94 ± 5.43	11.53 ± 0.117
2.	CH-5% NC	65.84 ± 2.63	18.90 ± 1.16	47.36 ± 1.51	84.45 ± 3.30	45.68 ± 3.80	10.22 ± 0.108
3.	CH-10% NC	70.00 ± 1.09	19.65 ± 0.42	63.11 ± 1.45	93.60 ± 2.53	66.98 ± 3.48	11.1 ± 0.12
4.	CH-1.5% MOF	66.72 ± 2.91	20.60 ± 1.61	25.65 ± 2.74	111.02 ± 1.86	37.81 ± 0.50	10.58 ± 0.27
5.	CH-2.5% MOF	68.36 ± 3.02	19.24 ± 1.57	37.37 ± 2.82	25.46 ± 2.53	46.31 ± 2.57	10.74 ± 0.275
6.	CH-5% NC-1.5% MOF	71.22 ± 3.21	16.49 ± 1.09	24.37 ± 1.80	110.60 ± 1.95	18.91 ± 4.01	9.518 ± 0.165
7.	CH-5% NC-2.5% MOF	74.99 ± 2.80	21.85 ± 1.05	36.5 ± 1.84	32.77 ± 1.21	34.91 ± 2.61	9.705 ± 0.036
8.	CH-10% NC-1.5% MOF	75.87 ± 3.12	22.00 ± 1.61	31.50 ± 1.40	109.62 ± 2.80	23.42 ± 3.22	9.89 ± 0.151
9.	CH-10% NC-2.5% MOF	77.88 ± 4.00	25.79 ± 1.10	38.68 ± 1.77	34.36 ± 1.86	26.31 ± 4.88	10.69 ± 0.058
10.	CH-10% NC-5% MOF	78.82 ± 1.59	18.85 ± 1.21	44.07 ± 2.37	21.82 ± 0.61	31.77 ± 0.507	10.74 ± 0.025

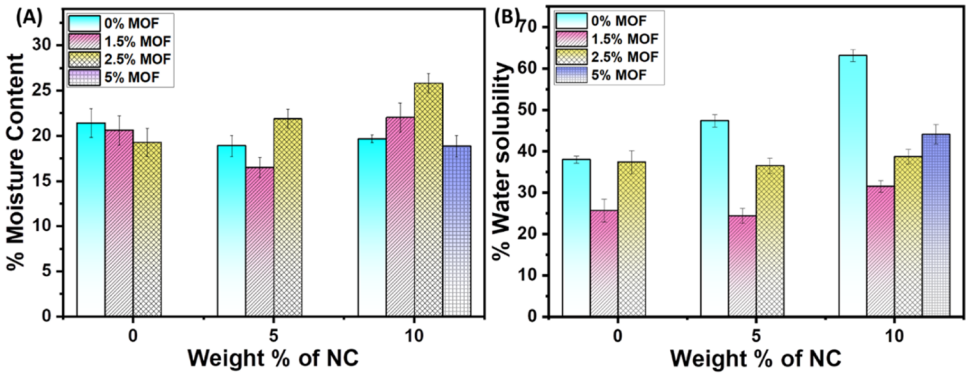

Figure 8. (A) Percentage of moisture content. (B) Percentage of water solubility of all synthesized films.

temperature range of 240−500 °C due to the decomposition of CH, NC, and gallic acid.

2.4. Properties of the Synthesized Films. *2.4.1. Determination of Moisture Content (MC), Water Solubility (WS), and Swelling Degree (SD).* The MC, WS, and SD are

https://doi.org/10.1021/acsomega.4c03847
ACS Omega 2024, 9, 35654−35665

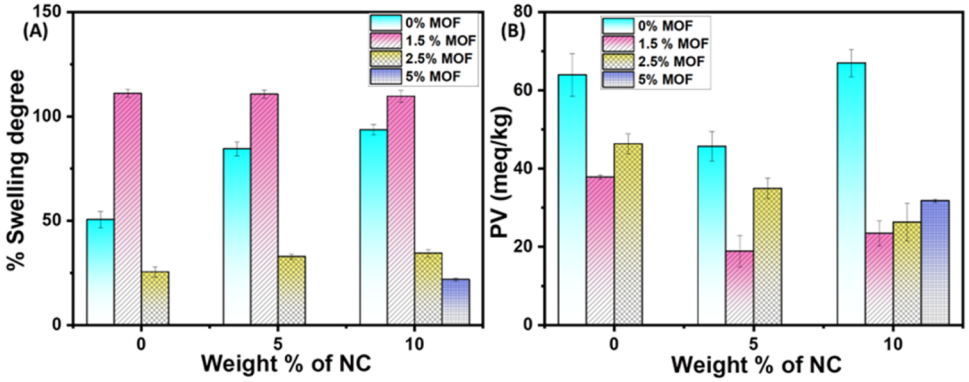

Figure 9. (A) Percentage of swelling degree. (B) Peroxide value (PV) of all synthesized films.

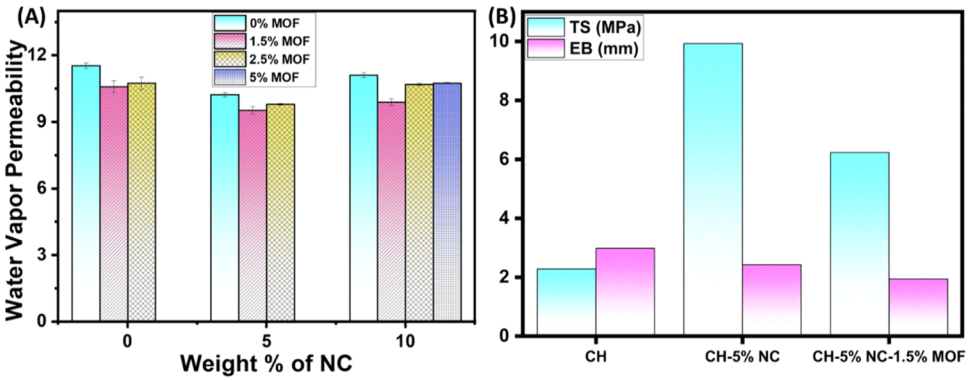

Figure 10. (A) Water vapor permeability (g h^{-1} m^{-2}) of all synthesized films. (B) Tensile strength (TS, MPa) and elongation at break (EB, mm) values of CH, CH-5% NC, and CH-5% NC-1.5% MOF films.

important factors for food packaging. These factors are vital as they affect the freshness, safety, and shelf life of packaged food.[59] Maintaining control over moisture levels, preventing materials from dissolving in water, and managing swelling are essential for ensuring packaging integrity and preserving food quality. All studies were carried out in triplicate (n = 3), and the standard deviation was calculated by Excel software. The mean ± standard deviation is used to express the data (Table 1).

Determination of MC is essential because microbial growth and destruction accelerate with an increase in the MC value.[60] It was observed that the MC of the film decreased after the incorporation of NC and the MOF in the CH film, caused by a higher degree of cross-linking and hydrogen-bonding interaction between chitosan, NC, and MOF (Figure 8A). The best combination of the components CH, NC, and MOF was present in the CH-5% NC-1.5% MOF film as it possesses a low MC value.

The WS of the film increased after the incorporation of NC in the CH film, which is attributed to the hydrogen-bonding interaction between free −OH of NC and water molecules. However, the WS decreased when the MOF was added to the CH film, as the MOF possesses a limited number of hydrogen binding sites. Subsequently, the WS decreased when the MOF was introduced in the CH−NC film due to the NC sites being bound to the MOF via hydrogen bonding, thereby reducing available sites for water binding. Furthermore, the plasticizer glycerol, with its hydrophilic properties, contributed to increased WS in the film.[61] Consequently, the addition of NC and the MOF to the CH film resulted in decreased WS, which may be attributed to hydrogen-bonding interactions between the components and limited opportunities for bond formation with water (Figure 8B).[62] Notably, the CH-5% NC-1.5% MOF film exhibited significantly lower WS compared with other films, emphasizing the effectiveness of this particular composition in minimizing WS.

The SD represents the water absorption capacity of the film.[63] When the NC was incorporated in the CH film, the SD of the film also increased due to an increase in the hydrogen binding sites (Figure 9A). This modification facilitated the enhanced adsorption of water molecules on the film's surface, consequently leading to an increase in SD. The SD sharply decreased from 50.5 ± 3.94% (CH-0% NC-0% MOF) to 21.82 ± 0.61% (CH-10% NC-5% MOF) because CH, NC, glycerol, and MOF highly interacted with each other via hydrogen bonding, which decreased the water absorption capacity.[63]

2.4.2. Oxygen Permeability. The transmission of oxygen can lead to the oxidation of food, resulting in the degradation of its quality, including undesirable odor, fading color, off-flavor, and nutrient loss.[64] Therefore, the permeability of oxygen is a crucial factor affecting the shelf life of preserved food. The oxygen permeability of the thin films was measured in terms of the peroxide value (PV) (meq/kg) (Table 1) using the sodium thiosulfate titration method (Table S1) (Figure 9B).[65] After the addition of 5% NC to the CH film and in the CH-MOF film, the PV decreased because of the high cross-linking between the components. When the concentrations of NC and the MOF were increased, aggregation occurred within the film, enhancing oxygen permeability and consequently increasing the PV.[66] The PV of the CH-5% NC-1.5% MOF film was determined to be 18.911 ± 4.009, demonstrating a close resemblance to the capped oil PV of 15.811 ± 1.135.

https://doi.org/10.1021/acsomega.4c03847
ACS Omega 2024, 9, 35654−35665

Table 2. Tensile Strength (TS), Elongation at Break (EB) Value, Color Space, and Color Difference (ΔE) of the Synthesized Films

s.no.	film	tensile strength (MPa)	elongation at break (mm)	lightness (L^*)	redness (a^*)	yellowness (b^*)	color difference (ΔE)
1.	chitosan (CH)	2.28	2.98	36.48	0.33	7.59	61.19
2.	CH-5% NC	9.93	2.42	34.10	1.35	9.30	63.74
3.	CH-5% NC-1.5% MOF	6.23	1.94	21.63	2.35	3.20	75.82

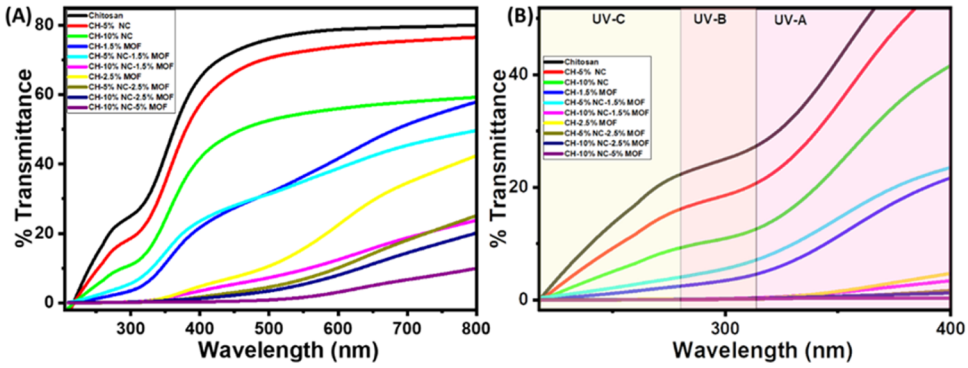

Figure 11. Light transmittance of all synthesized films (A) in the UV and visible region and (B) in the UV region only.

Conversely, the PV of the control, denoted by the open vial without film, was significantly elevated to 100.827 ± 3.747. This disparity suggests that the CH-5% NC-1.5% MOF film effectively shielded the oil from oxygen, as evidenced by the notably lower PV compared to that of the uncovered oil. These findings suggest that the synthesized film provides effective protection against oxygen, thereby preserving the oil's quality.

2.4.3. Water Vapor Permeability (WVP). WVP is a crucial property in food packaging, aiming to minimize moisture transfer between the food and its surroundings, thereby extending the food's shelf life by reducing the impact of external moisture. The result of WVP is shown in Table 1 and Figure 10A. The WVP of the CH film was found to be 11.53 ± 0.117 g h^{-1} m^{-2}. When NC and the MOF were incorporated into this film, the WVP decreased due to increased cross-linking between the components, preventing moisture transfer from the surroundings. As the concentration was increased, it led to the occurrence of aggregation, thereby enhancing the transfer of moisture through the film.[66] For instance, the WVP value for the CH-5% NC-1.5% MOF film was determined to be 9.518 ± 0.162 g h^{-1} m^{-2}, which was slightly low compared to other synthesized films and significantly lower than the open vial value of 50.08 ± 0.123 g h^{-1} m^{-2}. This combination was identified as the most suitable for food packaging, indicating its effectiveness in minimizing moisture transfer and extending the shelf life of packaged food products.

2.4.4. Mechanical Property. The results of the mechanical properties of films are shown in Figure 10B and Table 2. The tensile strength (TS) values for CH, CH-5% NC, and CH-5% NC-1.5% MOF films were 2.27, 9.27, and 6.23 MPa, respectively. The addition of NC to the CH film increased its strength, whereas the addition of the MOF to the CH−NC film decreased its strength. This suggests that the intermolecular hydrogen bonding between NC and CH was strong, but this strength decreased after the addition of the MOF, leading to a decrease in the film strength.[19]

Furthermore, the elongation at break (EB) values for CH, CH-5% NC, and CH-5% NC-1.5% MOF films were 2.98, 2.42, and 1.94 mm, respectively. The incorporation of NC and the MOF produced a rigid structure, restricting the relative motion of the CH film.[19]

2.4.5. Light Transmittance. Exposure to both visible and ultraviolet (UV) light can significantly affect food quality.[67] This impact was investigated through the light transmittance capabilities of a synthesized film, as demonstrated by UV−visible spectral analysis within the range of 200−800 nm (Figure 11A). The incorporation of NC and the MOF into the CH film resulted in a reduction in the light transmittance. As the concentrations of NC and MOF increased, the light transmittance decreased further due to the densification of the film. The films CH-2.5% MOF, CH-5% NC-2.5% MOF, CH-10% NC-2.5% MOF, and CH-10% NC-1.5% MOF demonstrated complete opacity within the UV−C (200−280 nm) and UV−B (280−315 nm) region,[68] whereas the CH-10% NC-5% MOF film showed no light transmission across the entire UV region (200−400 nm),[68] as illustrated in Figure 11B. Consequently, the incorporation of NC and the MOF resulted in a reduction in light transmission and an enhancement in light scattering, thereby diminishing the optical transmittance of the film.[69] Similar observations were also reported by other researchers using different composite films.[70−72] Films possessing barriers against ultraviolet and visible light can be employed to protect light-sensitive foods from light-induced oxidation.

2.4.6. Color Analysis. The color space values of the synthesized films are presented in Table 2. The white standard plate color space values were 97.41, −0.02, and 1.95 for lightness (L^*), redness (a^*), and yellowness (b^*) respectively. The color difference is represented by ΔE. The CH film showed a decrease in the L^* value and an increase in the a^* and b^* values compared to the white standard plate. When NC and MOF were added to the CH film, the film became darker, with an increased redness value and decreased lightness and yellowness values. Additionally, the ΔE value increased in the CH-5% NC-1.5% MOF film as compared with CH and CH-5% NC films. The findings are in good agreement with the enhancement of the color in the CH film after incorporating antioxidant components in the films.[73,74] It also supported the

https://doi.org/10.1021/acsomega.4c03847
ACS Omega 2024, 9, 35654−35665

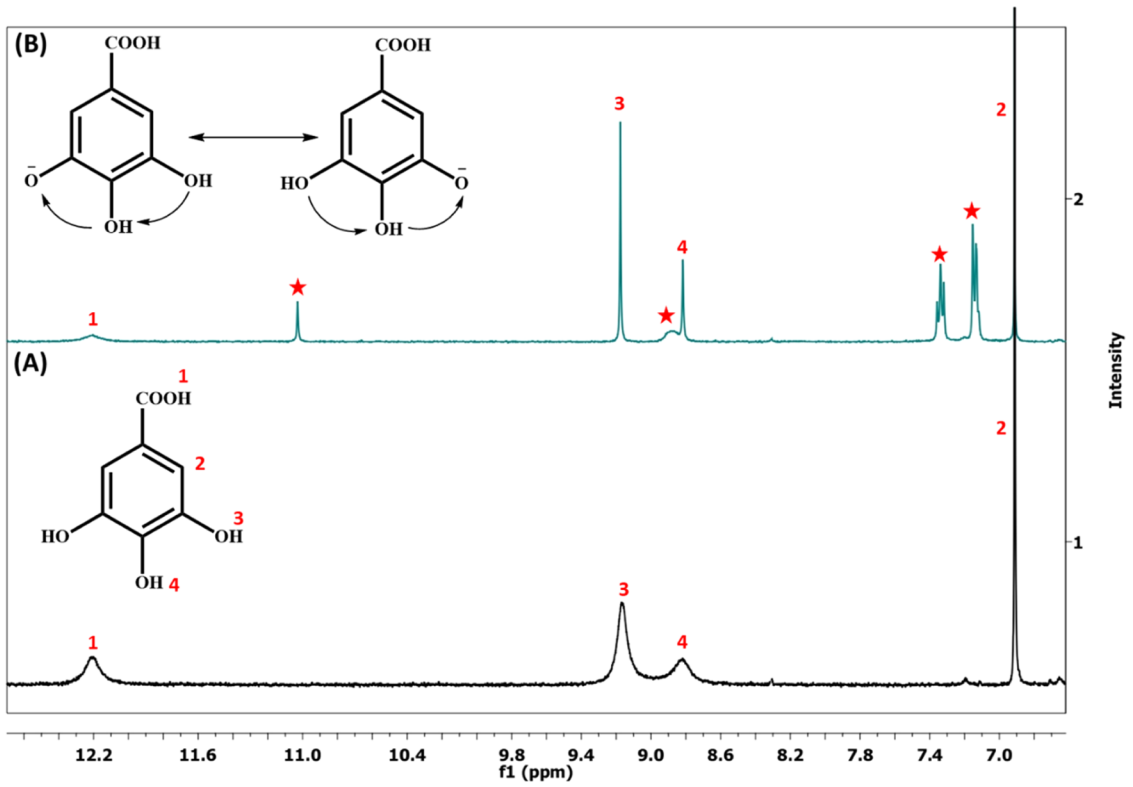

Figure 12. ^{1}H NMR spectra of (A) gallic acid and (B) gallic acid reaction with DPPH$^{\cdot}$ (DPPH$^{\cdot}$ signal represented by the star) in DMSO-d_6.

decreased light transmittance property of the CH-5% NC-1.5% MOF film due to the increased ΔE value.

2.4.7. Release Study of Synthesized Films. 2.4.7.1. Release of Gallic Acid from the Films. In the realm of food preservation, it is crucial to ensure consistent and controlled release of antioxidants from the packaging film. This is of utmost importance to maintain the quality and shelf life of food products. This sustained release mechanism plays a pivotal role in preserving food products by ensuring a prolonged and steady supply of antioxidants. Such an approach effectively safeguards the food against oxidative deterioration, prolongs its shelf life, and helps to retain its quality attributes over an extended storage period.[75] Different concentrations of ethanol are employed as stimulants for investigating release processes, depending on the food matrix. Specifically, a 10% ethanol concentration is deemed effective for studying alcoholic foods.[19] Release experiments were conducted using a 10% ethanol solution, aligned with parameters commonly applicable to alcoholic food matrices. The quantity of gallic acid released was assessed through the gallic acid standard curve with the utilization of the Folin−Ciocalteau reagent (Figure S13). The release studies were repeated three times, and the results are presented as the mean ± standard deviation. The film CH-2.5% MOF showed a rapid release of gallic acid for 33 days duration; after that, it became constant. This accelerated release behavior can be ascribed to the diminished interactions among the MOF, CH, and glycerol constituents, facilitating the rapid diffusion of gallic acid from the film matrix. After the addition of NC into the CH-MOF film, a noticeable deceleration in the release rate over an extended period was observed. This prolonged-release phenomenon can be attributed to enhanced hydrogen-bonding interactions among CH, NC, and MOF components within the film matrix. Upon an increase in the concentration of the MOF in the CH−NC−MOF film, a significant increase in the release quantity of gallic acid was observed. This phenomenon can be attributed to the increased concentration of the MOF, which can facilitate a greater release of gallic acid (Figure 13A). The findings from our study underscore that the active film CH-5% NC-1.5% MOF exhibited a sustained release of gallic acid over 52 days.

2.4.7.2. Release of Copper Ions from the Films. The quantification of copper (Cu) ions present in the simulants after 60 days was measured through a colorimetric assay, employing 3,3,5,5′-tetramethylbenzidine (TMB) as the chromogenic agent.[76] Upon addition of TMB to the aqueous solution containing a predetermined concentration of Cu ions, a light blue color was observed. The absorbance of the solution was recorded by using a UV−visible spectrophotometer at 897 nm. Subsequently, the calibration curve was established by plotting the absorbance at 897 nm against the known concentrations of the metal ion (Figure S14). However, this approach did not facilitate accurate measurement of the metal ion concentration in the simulants after 60 days. Therefore, the concentration of the copper ion was quantified by utilizing the inductively coupled plasma optical emission spectroscopy (ICP-OES) method. According to the ICP-OES analysis, the concentration of copper ions was detected to be below 0.01 ppm in the samples of CH-2.5% MOF, CH-1.5% MOF, CH-10% NC-1.5% MOF, CH-5% NC-1.5% MOF, and CH-5% NC-2.5% MOF films. In contrast, samples of CH-10% NC-2.5% MOF and CH-10% NC-5% MOF films exhibited copper ion concentrations of 0.04 ± 0.02 and 0.02 ± 0.003 ppm, respectively. These findings indicate that the observed level of ions is significantly lower than the permissible limit of copper ions.[77,78] Such levels do not pose any significant threat to human health. The findings of our studies suggest that the produced film effectively preserves alcoholic food, and there is

https://doi.org/10.1021/acsomega.4c03847
ACS Omega 2024, 9, 35654−35665

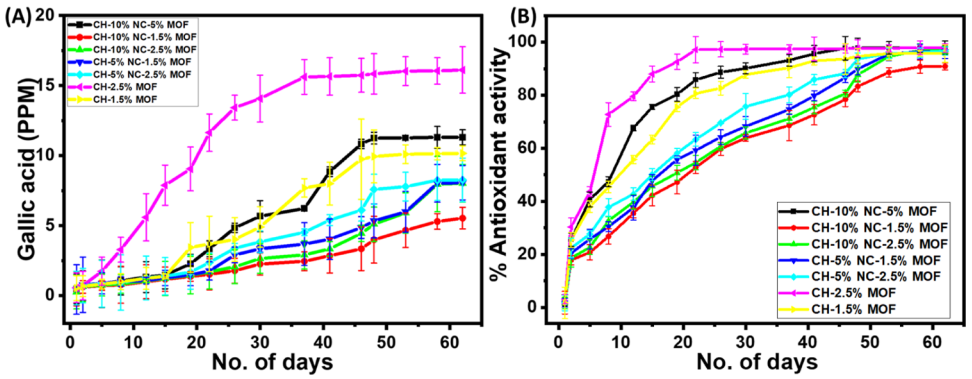

Figure 13. (A) Gallic acid release and (B) percentage ABTS$^{\dot{+}}$ antioxidant activity of the synthesized films.

Figure 14. Comparative study of the fresh-keeping performance of apple slices in the synthesized film CH-5% NC, CH-5% NC-1.5% MOF, and open slice.

no toxicity concern due to the presence of copper ions in the film.

2.4.8. Antioxidant Property. 2.4.8.1. Antioxidant Activity of Gallic Acid. The release of gallic acid in the food-simulating environment is very important owing to its antioxidant characteristics.[79] The antioxidant activity of gallic acid was verified using ^{1}H NMR spectroscopy using the DPPH radical (Figures S15−S17). In the ^{1}H NMR spectrum of gallic acid, peaks appeared at 12.21, 9.17, 8.82, and 6.90 ppm for the carboxylic acid proton, meta hydroxyl group proton, para-hydroxyl group proton, and ortho proton, respectively (Figure 12A). The signals for hydroxy protons were broad due to hydrogen-bonding interactions.[80] Upon adding the DPPH$^{\dot{}}$ solution to the gallic acid solution in a 1:1 ratio, the signals of the hydroxyl proton of gallic acid became sharp (Figure 12B). This sharpening suggests that one of the hydroxyl protons was lost upon a reaction with DPPH$^{\dot{}}$, and the remaining protons became delocalized due to their ortho configuration.[80] It was observed that DPPH was neutralized, leading to a faster color change from purple to brown. However, no new signals were detected in the NMR spectrum, indicating that no quinone was formed.

2.4.8.2. Antioxidant Properties of Prepared Films. After the antioxidant property of the gallic acid was confirmed, the antioxidant activity of the constituents leached from the film into the food simulant was evaluated using the ABTS and DPPH radical scavenging activity. The food stimulant exhibited antioxidant activity by both DPPH and ABTS radical scavenging activity. For the DPPH$^{\dot{}}$, the antioxidant activity was measured for 8 days, and the result is shown in Figure S18. However, ABTS$^{\dot{+}}$ is more sensitive to identifying the antioxidant activity due to faster reaction kinetics and high response against antioxidants.[81] Due to the advantage of ABTS$^{\dot{+}}$, the complete antioxidant study of the film was measured by ABTS$^{\dot{+}}$ radical scavenging activity. The duration of sustained antioxidant activity was observed in the CH-MOF film for less time as compared to other synthesized films. Incorporation of NC into the CH-MOF film resulted in prolonged antioxidant activity, attributed to enhanced component interaction leading to a gradual release of gallic acid. As the concentration of the MOF was increased, there was a corresponding enhancement in antioxidant activity (CH-2.5% MOF > CH-1.5% MOF and CH-10% NC-1.5% MOF < CH-10% NC-2.5% MOF < CH-10% NC-5% MOF) (Figure 13B). This escalation is attributed to the inherent property of the MOF to liberate substantial quantities of gallic acid, thereby amplifying the antioxidant efficacy. According to these results, it was observed that the film CH-5% NC-1.5% MOF displayed prolonged and substantial scavenging efficacy, which persisted for a noteworthy period of 52 days, and after that, it reached a steady state. This antioxidative film holds promise for extending the shelf life of food products over an extended period.

2.5. Real Sample Packaging Studies. The synthesized composite material was subsequently employed for the packaging of freshly cut apple slices. The freshness of the apple slice was assessed through a physical examination of samples. For packaging the slices, 12 packets were prepared, including six packets using CH-5% NC film and another six utilizing the CH-5% NC-1.5% MOF film. Each packet contained an apple slice, with one slice kept open as a control experiment. Over a specified period of 1, 2, 3, 5, 7, and 9 days,

https://doi.org/10.1021/acsomega.4c03847
ACS Omega 2024, 9, 35654−35665

the conditions of the apple slices were observed. Two packets were opened simultaneously, one from the CH-5% NC film group and the other from the CH-5% NC-1.5% MOF film group, and their physical conditions and freshness states were recorded. The browning phenomenon was observed in the exposed apple slice after 1 day, whereas discoloration occurred after 2 days in the slice packed in the CH-5% NC film. In contrast, the apple slice packed in the CH-5% NC-1.5% MOF film exhibited a markedly prolonged freshness, as only minor browning was noted after 9 days (Figure 14). The results indicate a significant improvement in the preservation of the apple slice in the CH-5% NC-1.5% MOF film over 9 day duration as compared to the control sample and CH-5% NC film-enclosed samples. This may be ascribed to the high oxygen barrier ability of this film, which inhibited oxidation by absorbing inside oxygen and reducing the oxidation of packed food. This active packaging material offers the advantage of providing a sustained release of antioxidants during storage. This sustained release is vital for maintaining antioxidant activity over an extended period, thereby effectively protecting the packaged food products from oxidative degradation.

2.6. Stability of the Film. After 9 months, the FTIR spectra of the synthesized CH, CH-5% NC, and CH-5% NC-1.5% MOF films were recorded. Similar FTIR spectra were observed when compared with the data of fresh films (Figures S19−S21). It indicated the presence of all components in the film without any decomposition. The physical appearance of the films was also observed to be similar to that of the fresh film, indicating that synthesized films were stable for a long period, such as 9 months.

2.7. Conclusions. We successfully synthesized a CH−NC−MOF active film by using different concentrations of NC (5, 10%) and MOF (1.5, 2.5, and 5%) in CH by a casting method. The best combination of a CH-5% NC-1.5% MOF film exhibited low oxygen permeability, WVP, MC, and WS as compared to other synthesized films. The CH-5% NC-1.5% MOF film demonstrated a high redness value and low lightness and yellowness values, which supported its low light transmittance value. It also exhibited the sustained release of antioxidants (gallic acid) for a long period of 52 days with high antioxidant activity in a 10% ethanol solution. Therefore, it exhibited good promise for preserving foodstuffs for a long duration of time. In the real sample packaging studies, the freshly cut apple slice remained fresh, even after 9 days. The synthesized film was also stable for a long period, such as 9 months. The results of the present study showed that the synthesized antioxidant film CH-5% NC-1.5% MOF can be used in the food packaging of fresh-cut fruits, vegetables, and alcoholic food, signifying a promising avenue for extending shelf life and maintaining the quality of perishable foods.

■ ASSOCIATED CONTENT

Supporting Information

The Supporting Information is available free of charge at https://pubs.acs.org/doi/10.1021/acsomega.4c03847.

Detailed experimental section and Figures S1−S21 (PDF)

■ AUTHOR INFORMATION

Corresponding Author

Pratibha Kumari − *Bioorganic Material Research Laboratory, Department of Chemistry, Deshbandhu College, University of Delhi, New Delhi 110019, India;* orcid.org/0000-0002-3830-3926; Email: pkumarichemistry@gmail.com

Author

Raveena − *Department of Chemistry, University of Delhi, New Delhi 110007, India; Bioorganic Material Research Laboratory, Department of Chemistry, Deshbandhu College, University of Delhi, New Delhi 110019, India*

Complete contact information is available at: https://pubs.acs.org/10.1021/acsomega.4c03847

Notes

The authors declare no competing financial interest.

■ ACKNOWLEDGMENTS

The authors are thankful to the Life Science Research Board, DRDO, Government of India, for the research funding (No. LSRB-388/FSH&ABB/2021). They are grateful to Deshbandhu College, University of Delhi, New Delhi, for providing research facilities. R. acknowledges CSIR for providing fellowship. The authors are also grateful to the Department of Chemistry, USIC, University of Delhi, New Delhi, and Material Research Centre (MNIT), Jaipur, India, for the characterization data.

■ REFERENCES

(1) Karn, R.; Prasad, E. *Packaging and Protective Packaging Market.* www.alliedmarketresearch.com.

(2) Sangroniz, A.; Zhu, J. B.; Tang, X.; Etxeberria, A.; Chen, E. Y. X.; Sardon, H. Packaging Materials with Desired Mechanical and Barrier Properties and Full Chemical Recyclability. *Nat. Commun.* **2019**, *10* (1), No. 3559.

(3) *Plastic Packaging Market Size, Share & Trends Analysis Report By Product (Rigid).* https://www.grandviewresearch.com/industry-analysis/industrial-packaging-market.

(4) Silva, F. A. G. S.; Dourado, F.; Gama, M.; Poças, F. Nanocellulose Bio-Based Composites for Food Packaging. *Nanomaterials* **2020**, *10* (10), No. 2041.

(5) Maitlo, G.; Ali, I.; Maitlo, H. A.; Ali, S.; Unar, I. N.; Ahmad, M. B.; Bhutto, D. K.; Karmani, R. K.; Naich, S. U.; Sajjad, R. U.; Ali, S.; Afridi, M. N. Plastic Waste Recycling, Applications, and Future Prospects for a Sustainable Environment. *Sustainability* **2022**, *14* (18), No. 11637.

(6) Bhuyan, M. S. Effects of Microplastics on Fish and in Human Health. *Front. Environ. Sci.* **2022**, *10*, No. 827289.

(7) Sharaby, M. R.; Soliman, E. A.; Abdel-Rahman, A. B.; Osman, A.; Khalil, R. Novel Pectin-Based Nanocomposite Film for Active Food Packaging Applications. *Sci. Rep.* **2022**, *12* (1), No. 20673.

(8) Miglioranza, B. M. G.; Spinelli, F. R.; Stoffel, F.; Piemolini-Barreto, L. T. Biodegradable Film for Raisins Packaging Application: Evaluation of Physico-Chemical Characteristics and Antioxidant Potential. *Food Chem.* **2021**, *365*, No. 130538.

(9) Wang, H.; Qian, J.; Ding, F. Emerging Chitosan-Based Films for Food Packaging Applications. *J. Agric. Food Chem.* **2018**, *66* (2), 395−413.

(10) Stefanowska, K.; Woźniak, M.; Dobrucka, R.; Ratajczak, I. Chitosan with Natural Additives as a Potential Food Packaging. *Materials* **2023**, *16* (4), No. 1579.

(11) Haghighi, H.; Licciardello, F.; Fava, P.; Siesler, H. W.; Pulvirenti, A. Recent Advances on Chitosan-Based Films for Sustainable Food Packaging Applications. *Food Packag. Shelf Life* **2020**, *26*, No. 100551.

(12) Ashfaq, A.; Khursheed, N.; Fatima, S.; Anjum, Z.; Younis, K. Application of Nanotechnology in Food Packaging: Pros and Cons. *J. Agric. Food Res.* **2022**, *7*, No. 100270.

(13) Le Gars, M.; Dhuiège, B.; Delvart, A.; Belgacem, M. N.; Missoum, K.; Bras, J. High-Barrier and Antioxidant Poly(Lactic Acid)/Nanocellulose Multilayered Materials for Packaging. *ACS Omega* **2020**, *5* (36), 22816−22826.
(14) Lai, C.; Zhang, S.; Chen, X.; Sheng, L. Nanocomposite Films Based on TEMPO-Mediated Oxidized Bacterial Cellulose and Chitosan. *Cellulose* **2014**, *21* (4), 2757−2772.
(15) Escamilla-García, M.; García-García, M. C.; Gracida, J.; Hernández-Hernández, H. M.; Granados-Arvizu, J. Á.; Di Pierro, P.; Regalado-González, C. Properties and Biodegradability of Films Based on Cellulose and Cellulose Nanocrystals from Corn Cob in Mixture with Chitosan. *Int. J. Mol. Sci.* **2022**, *23* (18), 10560.
(16) Sun, X.; Wang, Z.; Kadouh, H.; Zhou, K. The Antimicrobial, Mechanical, Physical and Structural Properties of Chitosan-Gallic Acid Films. *LWT–Food Sci. Technol.* **2014**, *57* (1), 83−89.
(17) Moreirinha, C.; Vilela, C.; Silva, N. H. C. S.; Pinto, R. J. B.; Almeida, A.; Rocha, M. A. M.; Coelho, E.; Coimbra, M. A.; Silvestre, A. J. D.; Freire, C. S. R. Antioxidant and Antimicrobial Films Based on Brewers Spent Grain Arabinoxylans, Nanocellulose and Feruloylated Compounds for Active Packaging. *Food Hydrocolloids* **2020**, *108*, No. 105836.
(18) Deshmukh, R. K.; Akhila, K.; Ramakanth, D.; Gaikwad, K. K. Guar Gum/Carboxymethyl Cellulose Based Antioxidant Film Incorporated with Halloysite Nanotubes and Litchi Shell Waste Extract for Active Packaging. *Int. J. Biol. Macromol.* **2022**, *201*, 1−13.
(19) Wang, X.; Xie, Y.; Ge, H.; Chen, L.; Wang, J.; Zhang, S.; Guo, Y.; Li, Z.; Feng, X. Physical Properties and Antioxidant Capacity of Chitosan/Epigallocatechin-3-Gallate Films Reinforced with Nano-Bacterial Cellulose. *Carbohydr. Polym.* **2018**, *179*, 207−220.
(20) Roy, S.; Rhim, J. W. Carboxymethyl Cellulose-Based Antioxidant and Antimicrobial Active Packaging Film Incorporated with Curcumin and Zinc Oxide. *Int. J. Biol. Macromol.* **2020**, *148*, 666−676.
(21) Badhani, B.; Sharma, N.; Kakkar, R. Gallic Acid: A Versatile Antioxidant with Promising Therapeutic and Industrial Applications. *RSC Adv.* **2015**, *5* (35), 27540−27557.
(22) Almeida, T.; Karamysheva, A.; Valente, B. F. A.; Silva, J. M.; Braz, M.; Almeida, A.; Silvestre, A. J. D.; Vilela, C.; Freire, C. S. R. Biobased Ternary Films of Thermoplastic Starch, Bacterial Nanocellulose and Gallic Acid for Active Food Packaging. *Food Hydrocolloids* **2023**, *144*, No. 108934.
(23) Zhang, X.; Liu, J.; Qian, C.; Kan, J.; Jin, C. Effect of Grafting Method on the Physical Property and Antioxidant Potential of Chitosan Film Functionalized with Gallic Acid. *Food Hydrocolloids* **2019**, *89*, 1−10.
(24) Rui, L.; Xie, M.; Hu, B.; Zhou, L.; Yin, D.; Zeng, X. A Comparative Study on Chitosan/Gelatin Composite Films with Conjugated or Incorporated Gallic Acid. *Carbohydr. Polym.* **2017**, *173*, 473−481.
(25) Wang, Y.; Du, H.; Xie, M.; Ma, G.; Yang, W.; Hu, Q.; Pei, F. Characterization of the Physical Properties and Biological Activity of Chitosan Films Grafted with Gallic Acid and Caffeic Acid: A Comparison Study. *Food Packag. Shelf Life* **2019**, *22*, No. 100401.
(26) Liu, J.; Liu, S.; Zhang, X.; Kan, J.; Jin, C. Effect of Gallic Acid Grafted Chitosan Film Packaging on the Postharvest Quality of White Button Mushroom (*Agaricus bisporus*). *Postharvest Biol. Technol.* **2019**, *147*, 39−47.
(27) Azhar, B.; Angkawijaya, A. E.; Santoso, S. P.; Gunarto, C.; Ayucitra, A.; Go, A. W.; Tran-Nguyen, P. L.; Ismadji, S.; Ju, Y. H. Aqueous Synthesis of Highly Adsorptive Copper−Gallic Acid Metal−Organic Framework. *Sci. Rep.* **2020**, *10* (1), No. 19212.
(28) Sharma, S.; Mittal, D.; Verma, A. K.; Roy, I. Copper-Gallic Acid Nanoscale Metal-Organic Framework for Combined Drug Delivery and Photodynamic Therapy. *ACS Appl. Bio Mater.* **2019**, *2* (5), 2092−2101.
(29) Bian, H.; Yang, Y.; Tu, P.; Chen, J. Y. Value-Added Utilization of Wheat Straw: From Cellulose and Cellulose Nanofiber to All-Cellulose Nanocomposite Film. *Membranes* **2022**, *12* (5), No. 475.
(30) Saito, T.; Nishiyama, Y.; Putaux, J. L.; Vignon, M.; Isogai, A. Homogeneous Suspensions of Individualized Microfibrils from TEMPO-Catalyzed Oxidation of Native Cellulose. *Biomacromolecules* **2006**, *7* (6), 1687−1691.
(31) da Silva Perez, D.; Montanari, S.; Vignon, M. R. TEMPO-Mediated Oxidation of Cellulose III. *Biomacromolecules* **2003**, *4* (5), 1417−1425.
(32) Coseri, S.; Biliuta, G.; Zemljič, L. F.; Srndovic, J. S.; Larsson, P. T.; Strnad, S.; Kreže, T.; Naderi, A.; Lindström, T. One-Shot Carboxylation of Microcrystalline Cellulose in the Presence of Nitroxyl Radicals and Sodium Periodate. *RSC Adv.* **2015**, *5* (104), 85889−85897.
(33) Zeng, J.; Zeng, Z.; Cheng, Z.; Wang, Y.; Wang, X.; Wang, B.; Gao, W. Cellulose Nanofibrils Manufactured by Various Methods with Application as Paper Strength Additives. *Sci. Rep.* **2021**, *11* (1), No. 11918.
(34) Chieng, B. W.; Lee, S. H.; Ibrahim, N. A.; Then, Y. Y.; Loo, Y. Y. Isolation and Characterization of Cellulose Nanocrystals from Oil Palm Mesocarp Fiber. *Polymers* **2017**, *9* (8), No. 355.
(35) Alvarado, D. R.; Argyropoulos, D. S.; Scholle, F.; Peddinti, B. S. T.; Ghiladi, R. A. A Facile Strategy for Photoactive Nanocellulose-Based Antimicrobial Materials. *Green Chem.* **2019**, *21* (12), 3424−3435.
(36) Maiti, S.; Jayaramudu, J.; Das, K.; Reddy, S. M.; Sadiku, R.; Ray, S. S.; Liu, D. Preparation and Characterization of Nano-Cellulose with New Shape from Different Precursor. *Carbohydr. Polym.* **2013**, *98* (1), 562−567.
(37) Arnata, I. W.; Suprihatin, S.; Fahma, F.; Richana, N.; Sunarti, T. C. Cationic Modification of Nanocrystalline Cellulose from Sago Fronds. *Cellulose* **2020**, *27* (6), 3121−3141.
(38) Jiang, F.; Han, S.; Hsieh, Y. L. Controlled Defibrillation of Rice Straw Cellulose and Self-Assembly of Cellulose Nanofibrils into Highly Crystalline Fibrous Materials. *RSC Adv.* **2013**, *3* (30), 12366−12375.
(39) Queiroz, M. F.; Melo, K. R. T.; Sabry, D. A.; Sassaki, G. L.; Rocha, H. A. O. Does the Use of Chitosan Contribute to Oxalate Kidney Stone Formation? *Mar. Drugs* **2015**, *13* (1), 141−158.
(40) Martins, C. S.; Morgado, D. L.; Assi, O. B. G. Cashew Gum-Chitosan Blended Films: Spectral, Mechanical and Surface Wetting Evaluations. *Macromol. Res.* **2016**, *24* (8), 691−697.
(41) Sun, L.; Sun, J.; Chen, L.; Niu, P.; Yang, X.; Guo, Y. Preparation and Characterization of Chitosan Film Incorporated with Thinned Young Apple Polyphenols as an Active Packaging Material. *Carbohydr. Polym.* **2017**, *163*, 81−91.
(42) Leceta, I.; Guerrero, P.; De La Caba, K. Functional Properties of Chitosan-Based Films. *Carbohydr. Polym.* **2013**, *93*, 339−346.
(43) Branca, C.; D'Angelo, G.; Crupi, C.; Khouzami, K.; Rifici, S.; Ruello, G.; Wanderlingh, U. Role of the OH and NH Vibrational Groups in Polysaccharide-Nanocomposite Interactions: A FTIR-ATR Study on Chitosan and Chitosan/Clay Films. *Polymer* **2016**, *99*, 614−622.
(44) Biswal, H. S.; Shirhatti, P. R.; Wategaonkar, S. O-H···O versus O-H···S Hydrogen Bonding. 2. Alcohols and Thiols as Hydrogen Bond Acceptors. *J. Phys. Chem. A* **2010**, *114* (26), 6944−6955.
(45) Momtaz, M.; Momtaz, E.; Mehrgardi, M. A.; Momtaz, F.; Narimani, T.; Poursina, F. Preparation and Characterization of Gelatin/Chitosan Nanocomposite Reinforced by NiO Nanoparticles as an Active Food Packaging. *Sci. Rep.* **2024**, *14* (1), No. 519.
(46) Hai, T. A. P.; Sugimoto, R. Fluorescence Control of Chitin and Chitosan Fabricated: Via Surface Functionalization Using Direct Oxidative Polymerization. *RSC Adv.* **2018**, *8* (13), 7005−7013.
(47) Saeed, A. M.; Taha, A. G.; Dardeer, H. M.; Aly, M. F. One-Pot Synthesis of Novel Chitosan-Salicylaldehyde Polymer Composites for Ammonia Sensing. *Sci. Rep.* **2024**, *14* (1), No. 239.
(48) Pereda, M.; Ponce, A. G.; Marcovich, N. E.; Ruseckaite, R. A.; Martucci, J. F. Chitosan-Gelatin Composites and Bi-Layer Films with Potential Antimicrobial Activity. *Food Hydrocolloids* **2011**, *25* (5), 1372−1381.

https://doi.org/10.1021/acsomega.4c03847
ACS Omega 2024, 9, 35654−35665

(49) Rubentheren, V.; Ward, T. A.; Chee, C. Y.; Nair, P. Physical and Chemical Reinforcement of Chitosan Film Using Nanocrystalline Cellulose and Tannic Acid. *Cellulose* **2015**, *22* (4), 2529−2541.
(50) Zhang, P.; Zhao, Y.; Shi, Q. Characterization of a Novel Edible Film Based on Gum Ghatti: Effect of Plasticizer Type and Concentration. *Carbohydr. Polym.* **2016**, *153*, 345−355.
(51) Sahoo, R.; Sundara, R.; Venkatachalam, S. Silver Nanowires Coated Nitrocellulose Paper for High-Efficiency Electromagnetic Interference Shielding. *ACS Omega* **2022**, *7* (45), 41426−41436.
(52) Grigioni, I.; Polo, A.; Nomellini, C.; Vigni, L.; Poma, A.; Dozzi, M. V.; Selli, E. Nature of Charge Carrier Recombination in CuWO4 Photoanodes for Photoelectrochemical Water Splitting. *ACS Appl. Energy Mater.* **2023**, *6* (19), 10020−10029.
(53) Tamilselvan, M.; Byregowda, A.; Su, C. Y.; Tseng, C. J.; Bhattacharyya, A. J. Planar Heterojunction Solar Cell Employing a Single-Source Precursor Solution-Processed Sb2S3 Thin Film as the Light Absorber. *ACS Omega* **2019**, *4* (7), 11380−11387.
(54) Qing, H.; Fan, S.; Liu, Y.; Li, C.; Meng, J.; Yang, M.; Xiao, Z. Thin-Film Composite (TFC) Polydimethylsiloxane (PDMS) Membrane with High Crosslinking Density Fabricated by Coaxial Electrospray for a High Flux. *Ind. Eng. Chem. Res.* **2023**, *62* (2), 1112−1120.
(55) Jahed, E.; Khaledabad, M. A.; Almasi, H.; Hasanzadeh, R. Physicochemical Properties of Carum Copticum Essential Oil Loaded Chitosan Films Containing Organic Nanoreinforcements. *Carbohydr. Polym.* **2017**, *164*, 325−338.
(56) Rizal, S.; Yahya, E. B.; Abdul Khalil, H. P. S.; Abdullah, C. K.; Marwan, M.; Ikramullah, I.; Muksin, U. Preparation and Characterization of Nanocellulose/Chitosan Aerogel Scaffolds Using Chemical-Free Approach. *Gels* **2021**, *7* (4), No. 246.
(57) Gan, P. G.; Sam, S. T.; Abdullah, M. F.; Omar, M. F. Thermal Properties of Nanocellulose-Reinforced Composites: A Review. *J. Appl. Polym. Sci.* **2020**, *137*, No. 48544.
(58) Zayed, M. F.; Eisa, W. H.; Anis, B. Gallic Acid-Assisted Growth of Cuprous Oxide within Polyvinyl Alcohol; a Separable Catalyst for Oxidative and Reductive Degradation of Water Pollutants. *J. Cleaner Prod.* **2021**, *279*, No. 123826, DOI: 10.1016/j.jclepro.2020.123826.
(59) Sutharsan, J.; Boyer, C. A.; Zhao, J. Physicochemical Properties of Chitosan Edible Films Incorporated with Different Classes of Flavonoids. *Carbohydr. Polym. Technol. Appl.* **2022**, *4*, No. 100232.
(60) Alp, D.; Bulantekin, Ö. The Microbiological Quality of Various Foods Dried by Applying Different Drying Methods: A Review. *Eur. Food Res. Technol.* **2021**, *247*, 1333−1343.
(61) Wang, X.; Ullah, N.; Sun, X.; Guo, Y.; Chen, L.; Li, Z.; Feng, X. Development and Characterization of Bacterial Cellulose Reinforced Biocomposite Films Based on Protein from Buckwheat Distiller's Dried Grains. *Int. J. Biol. Macromol.* **2017**, *96*, 353−360.
(62) Jafari, H.; Pirouzifard, M. K.; Khaledabad, M. A.; Almasi, H. Effect of Chitin Nanofiber on the Morphological and Physical Properties of Chitosan/Silver Nanoparticle Bionanocomposite Films. *Int. J. Biol. Macromol.* **2016**, *92*, 461−466.
(63) Khan, A.; Khan, R. A.; Salmieri, S.; Le Tien, C.; Riedl, B.; Bouchard, J.; Chauve, G.; Tan, V.; Kamal, M. R.; Lacroix, M. Mechanical and Barrier Properties of Nanocrystalline Cellulose Reinforced Chitosan Based Nanocomposite Films. *Carbohydr. Polym.* **2012**, *90* (4), 1601−1608.
(64) Pires, J.; de Paula, C. D.; Souza, V. G. L.; Fernando, A. L.; Coelhoso, I. Understanding the Barrier and Mechanical Behavior of Different Nanofillers in Chitosan Films for Food Packaging. *Polymers* **2021**, *13* (5), No. 721.
(65) Hesham, R. L.; Celine, M.; Celestine, R. Analysis of Different Namibian Traditional Oils against Commercial Sunflower and Olive Oils. *Afr. J. Food Sci.* **2015**, *9* (6), 372−379.
(66) Soni, B.; Hassan, E. B.; Schilling, M. W.; Mahmoud, B. Transparent Bionanocomposite Films Based on Chitosan and TEMPO-Oxidized Cellulose Nanofibers with Enhanced Mechanical and Barrier Properties. *Carbohydr. Polym.* **2016**, *151*, 779−789.
(67) Arfat, Y. A.; Ahmed, J.; Hiremath, N.; Auras, R.; Joseph, A. Thermo-Mechanical, Rheological, Structural and Antimicrobial Properties of Bionanocomposite Films Based on Fish Skin Gelatin and Silver-Copper Nanoparticles. *Food Hydrocolloids* **2017**, *62*, 191−202.
(68) Kriechbaum, K.; Bergström, L. Antioxidant and UV-Blocking Leather-Inspired Nanocellulose-Based Films with High Wet Strength. *Biomacromolecules* **2020**, *21* (5), 1720−1728.
(69) Fernandes, S. C. M.; Oliveira, L.; Freire, C. S. R.; Silvestre, A. J. D.; Neto, C. P.; Gandini, A.; Desbriéres, J. Novel Transparent Nanocomposite Films Based on Chitosan and Bacterial Cellulose. *Green Chem.* **2009**, *11* (12), 2023−2029.
(70) Franco, T. S.; Amezcua, R. M. J.; Rodrìguez, A. V.; Enriquez, S. G.; Urquíza, M. R.; Mijares, E. M.; de Muniz, G. B. Carboxymethyl and Nanofibrillated Cellulose as Additives on the Preparation of Chitosan Biocomposites: Their Influence Over Films Characteristics. *J. Polym. Environ.* **2020**, *28* (2), 676−688.
(71) Kusmono; Wildan, M. W.; Lubis, F. I. Fabrication and Characterization of Chitosan/Cellulose Nanocrystal/Glycerol Bio-Composite Films. *Polymers* **2021**, *13* (7), No. 1096.
(72) Wardana, A. A.; Koga, A.; Tanaka, F.; Tanaka, F. Antifungal Features and Properties of Chitosan/Sandalwood Oil Pickering Emulsion Coating Stabilized by Appropriate Cellulose Nanofiber Dosage for Fresh Fruit Application. *Sci. Rep.* **2021**, *11* (1), No. 18412.
(73) Liu, J.; Meng, C. G.; Liu, S.; Kan, J.; Jin, C. H. Preparation and Characterization of Protocatechuic Acid Grafted Chitosan Films with Antioxidant Activity. *Food Hydrocolloids* **2017**, *63*, 457−466.
(74) Aljawish, A.; Muniglia, L.; Klouj, A.; Jasniewski, J.; Scher, J.; Desobry, S. Characterization of Films Based on Enzymatically Modified Chitosan Derivatives with Phenol Compounds. *Food Hydrocolloids* **2016**, *60*, 551−558.
(75) Westlake, J. R.; Tran, M. W.; Jiang, Y.; Zhang, X.; Burrows, A. D.; Xie, M. Biodegradable Active Packaging with Controlled Release: Principles, Progress, and Prospects. *ACS Food Sci. Technol.* **2022**, *2* (8), 1166−1183.
(76) Chen, L.; Li, Y.; Sun, P.; Chen, H.; Li, H.; Liu, J.; Chen, Z.; Wang, B. A Facile Colorimetric Method for Ultra-Rapid and Sensitive Detection of Copper Ions in Water. *J. Inorg. Organomet. Polym. Mater.* **2022**, *32* (7), 2473−2481.
(77) Javed, M.; Usmani, N.; Javed, M. Uptake of Heavy Metals by Channa Punctatus from Sewage-Fed Aquaculture Pond of Panethi, Aligarh. *Glob. J. Eng. Res. C* **2012**, *12* (2), 27−34.
(78) Gaetke, L. M.; Chow-Johnson, H. S.; Chow, C. K. Copper: Toxicological Relevance and Mechanisms. *Arch. Toxicol.* **2014**, *88*, 1929−1938.
(79) Jacobs, E.; Chambin, O.; Debeaufort, F.; Benbettaieb, N. Synergic versus Antagonist Effects of Rutin on Gallic Acid or Coumarin Incorporated into Chitosan Active Films: Impacts on Their Release Kinetics and Antioxidant Activity. *Antioxidants* **2023**, *12* (11), No. 1934.
(80) López-Martínez, L. M.; Santacruz-Ortega, H.; Navarro, R. E.; Sotelo-Mundo, R. R.; González-Aguilar, G. A. A 1H NMR Investigation of the Interaction between Phenolic Acids Found in Mango (Manguifera Indica Cv Ataulfo) and Papaya (Carica Papaya Cv Maradol) and 1,1-Diphenyl-2-Picrylhydrazyl (DPPH) Free Radicals. *PLoS One* **2015**, *10* (11), No. e0140242.
(81) Floegel, A.; Kim, D. O.; Chung, S. J.; Koo, S. I.; Chun, O. K. Comparison of ABTS/DPPH Assays to Measure Antioxidant Capacity in Popular Antioxidant-Rich US Foods. *J. Food Compos. Anal.* **2011**, *24* (7), 1043−1048.

https://doi.org/10.1021/acsomega.4c03847
ACS Omega 2024, 9, 35654−35665